1993

Infrared Emission Spectroscopy with Transient Cooling

Randy J. Pell

Charles E. Miller
Haverford College

Bruce R. Kowalski

James B. Callis

Infrared Emission Spectroscopy with Transient Cooling

RANDY J. PELL,* CHARLES E. MILLER,† BRUCE R. KOWALSKI, and JAMES B. CALLIS

Department of Chemistry, Laboratory for Chemometrics, Center for Process Analytical Chemistry, University of Washington, Seattle, Washington 98195

A new approach for collection of infrared spectral data from optically opaque materials is explored. This approach has previously been introduced in the literature and is known as transient infrared transmission spectroscopy (TIRTS). The front surface of a hot sample is transiently cooled with a jet of cold gas, and the ratio of the spectrum measured after cooling to that measured before cooling is shown to closely resemble a transmission spectrum. This report provides for a more theoretical understanding of the experiments than provided by previous workers, making use of unsteady-state heat flow calculations, harmonic oscillator modeling, and radiation transfer theory. Experimental data are collected from a solid polymer sample and two viscous liquid samples. The position of the spectral features for the emission measurements corresponds with transmission measurements, with some saturation of the more intense spectral features noted. Faster scanning instrumentation, proper pulse scan synchronization, or rotation of solid samples, as demonstrated by previous workers, may resolve the saturation problem.

Index Headings: **Infrared; Emission; Transient cooling; TIRTS.**

INTRODUCTION

There are two major experimental difficulties that have limited the usefulness of infrared emission spectroscopy as an analytical technique. The first is discrimination of weak sample emission from an overwhelming background emission signal. The sample must be heated or cooled to distinguish it from the surroundings, and furthermore it must be at a temperature different from the detector. For conventional infrared emission spectroscopy, this problem is usually overcome by heating the back surface of the sample. Alternatively, Chase[1] and Low and Coleman[2] have demonstrated that cooling the sample below the detector temperature is also a possibility since, in theory, only a temperature difference between sample and detector is needed. Nevertheless, Fourier transform techniques and cooled detectors have allowed this experimental problem to be overcome to a great extent.

The second major difficulty is the sampling of optically opaque materials. As a uniformly heated sample becomes opaque, the absorptance approaches 1 and, according to Kirchoff's law, the emittance must also approach 1, provided that the absorptive losses are due to absorption only and are not the result of reflection or scattering effects.[3] As a result, any potential spectral emission features are obscured for thick, uniformly heated samples, due to the ever increasing background.[4] In order to deal with opaque materials Koga *et al.* proposed front-surface heating of the sample.[5] More recently, continuous and pulse laser excitation[6–8] and hot gas stream excitation[9] have been used to produce a thin layer of above-ambient-temperature material on the surface of opaque samples. This approach solves the problems of discrimination against a background, loss of contrast, and distortion of band shapes due to opacity.

Many process analysis problems involve materials already above ambient temperatures; thus, a technique that further heats the sample may be of limited use. There are also concerns of safety in a process situation, as well as sample damage, associated with laser heating. An alternative approach demonstrated by Jones and McClelland involves the front-surface cooling of a hot sample and thus the creation of a temperature gradient in the reverse fashion of the laser heating experiment.[10] By measuring the spectrum before and after cooling of the surface and ratioing the two measurements, not only does one obtain a transmission-like spectrum but also selective reflections at the surface are eliminated because an optically opaque sample has been used as a reference.[11] The bulk sample then becomes the "source," while the cooled surface layer becomes the "sample." The degree to which spectral features may be discerned will depend upon the "steepness" of the induced temperature gradient, which is a function of the thermal properties of the material, the properties of the coolant, the pulse duration, and the scan pulse synchronization precision.

The work described herein considers the effects of unsteady heat flow, as well as radiative transfer from the damped harmonic oscillator, in order to better understand the experimental observation.

THEORY

Theoretical considerations of the behavior of infrared emission spectra collected with transient cooling must begin with a model for the temperature distribution in a material under unsteady-state conditions. The experimental situation that will be considered is shown in Fig. 1. A semi-transparent material of thickness L is attached to a metal backing. The initial temperature is T_i, and at time zero the surface temperature is suddenly lowered and maintained at T_0. The temperature distribution, $T(x, \tau)$ will be a function of position, x, and time, τ. According to Holman,[12] the differential equation describing the temperature distribution is

$$\frac{\partial^2 T}{\partial x^2} = \frac{1}{\alpha}\frac{\partial T}{\partial \tau} \tag{1}$$

where α is the thermal diffusivity. Given the following boundary and initial conditions:

Received 1 March 1993; revision received 25 June 1993.

* Author to whom correspondence should be sent. Current address: Analytical Sciences Laboratory, The Dow Chemical Company, 1897D Building, Midland, MI 48667.

† Current address: DuPont Polymers, P.O. Box 1089, Bldg. 10, Orange, TX 77631-1089.

0003-7028/93/4712-2064$2.00/0

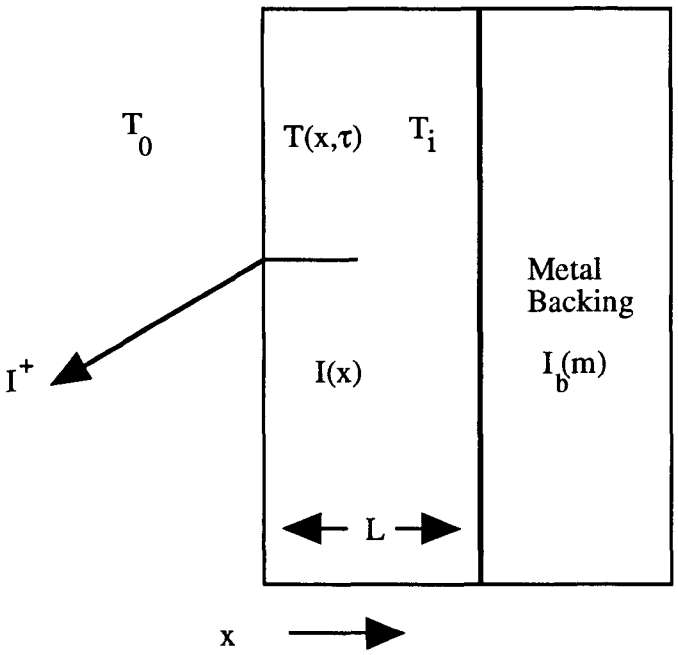

FIG. 1. Experimental situation considered for theoretical development.

$$T(x, 0) = T_i \tag{2}$$

$$T(0, \tau) = T_0 \text{ for } \tau > 0, \tag{3}$$

Eq. 1 may be solved by the Laplace-transform technique and is given as

$$\frac{T(x, \tau) - T_0}{T_i - T_0} = \text{erf}\left[\frac{x}{2\sqrt{\alpha\tau}}\right] \tag{4}$$

where the Gauss error function is defined as

$$\text{erf}\left[\frac{x}{2\sqrt{\alpha\tau}}\right] = \frac{2}{\sqrt{\pi}} \int_0^{x/2\sqrt{\alpha\tau}} e^{-\eta^2}\, d\eta. \tag{5}$$

Given the thermal diffusivity, α, the initial surface temperature, T_i, and the temperature, T_0, of the coolant gas, the temporal and spatial behavior of the temperature, $T(x, \tau)$, may be calculated. This temperature distribution may then be used in conjunction with radiative transfer theory to develop a model for the spectral observations from an IRE-TC (infrared emission with transient cooling) experiment.

The radiation transfer equation may be written as

$$\frac{dI_\nu(x)}{dx} = -k_\nu[n_\nu^2 I_{b\nu}(x) - I_\nu(x)] \tag{6}$$

where $I_{b\nu}(x)$ is the radiance given by the Planck blackbody function at temperature $T(x)$, $I_\nu(x)$ is the radiance at position x (see Fig. 1), k_ν is the spectral absorption coefficient, and n is the refractive index of the material.[13] The subscript ν indicates wavenumber-dependent quantities which are implied in the remaining equations. Only normal incidence light is assumed, and thus no angular dependence is included in Eq. 6. Equation 6 states that the change in radiance with distance in a sample is the difference between the radiation emitted (first term on the right) and the radiation absorbed (second term on the right). Given the appropriate boundary conditions,[13] Eq. 6 may be solved and written as

$$I_\nu^+(0) = (1 - p_1)\left[\frac{n_0}{n}\right]^2 \beta \times \left\{(1 - p_2)n^2 I_b(m)e^{-kL} + \int_0^L n^2 I_b(x)k[e^{-kx} + p_2 e^{-k[2L-x]}]\, dx\right\} \tag{7}$$

where $\beta = (1 - p_1 p_2 \exp[-2kL])^{-1}$; I^+ is the exiting radiance (see Fig. 1); $I_b(m)$ denotes the contribution by the metal backing at temperature $T(m)$, given by Planck's equation; p_1 and p_2 are the front-surface and back-surface reflectivities; and n, the index of refraction of the film, is related to n_0, the index of refraction of the boundary material (air), via Snell's law.

Equation 7 is a basic equation that may be solved for many experimental situations. This equation may be used in conjunction with the temperature gradient information from Eq. 4 to compute the spectral behavior under different experimental conditions. Note that if k, n, and $I_b(m)$ are known and I^+ is measured, then Eq. 7 may be treated as a nonlinear Fredholm integral equation of the first kind for the unknown function $I_b(x)$, and thus the temperature distribution may be computed from the measured spectrum. Hommert *et al.* have used this approach to determine the temperature gradient in slabs of cooling glass.[14] For simulation of spectral features, the integral from Eq. 7 is solved numerically with the positional dependence of $I_b(x)$ given by the imposed temperature gradient. For the purpose of this paper, k_ν will be assumed to be independent of temperature. If there is no temperature gradient then $I_b(x) = I_b(m) = I_b$, and Eq. 7 may be solved analytically, giving

$$I^+ = \frac{(1 - p_1)(1 - p_2 e^{-2kL})}{(1 - p_1 p_2 e^{-2kL})} I_b n_0^2 \tag{8}$$

or for the emittance, ϵ, which is the ratio of the measured signal to a blackbody signal at the same temperature, the functional form is

$$\epsilon = \frac{(1 - p_1)(1 - p_2 e^{-2kL})}{(1 - p_1 p_2 e^{-2kL})}. \tag{9}$$

Equation 8 may be used as a check of the integration of Eq. 7 for the zero-gradient experiment. For a given temperature gradient, I^+ from Eq. 7 may be ratioed to I^+ from Eq. 8 to simulate an IRE-TC experiment.

In order to simulate the spectral behavior, an isothermal harmonic oscillator model is used to calculate the absorption index and refractive index optical constant spectra as outlined by Hvistendahl *et al.*[11] Briefly, assuming one band in the infrared and several in the visible, the harmonic oscillator model simplifies to

$$n^2 - \kappa^2 = n_\nu^2 + \frac{B(\nu_0^2 - \nu^2)}{(\nu_0^2 - \nu^2)^2 + \gamma\nu^2} \tag{10}$$

$$2n\kappa = \frac{B\gamma\nu}{(\nu_0^2 - \nu^2)^2 + \gamma^2\nu^2} \tag{11}$$

where n_ν is the refractive index of the sample extrapolated from the visible; n and κ are the optical constant spectra calculated as a function of frequency, ν; B is the oscillator strength; γ is the damping coefficient; and ν_0 is the resonance frequency. The front-surface reflectivity, needed in Eq. 7, is given by

$$p_1 = \frac{(n_2 - n_1)^2 + \kappa^2}{(n_2 + n_1)^2 + \kappa^2} \tag{12}$$

where an air/material interface is assumed, giving $n_1 = 1$, and the back-surface reflectivity, p_2, is assumed to be equal to one. Equation 13 will relate the computed absorption index spectrum, κ, to the spectral absorption coefficient, k, as

$$k = 4\pi\nu\kappa. \tag{13}$$

In summary, the thermal properties define the temperature gradient information which is used to describe the positional dependence of $I_b(x)$ in the integral of Eq. 7. The harmonic oscillator parameters will define the optical constant spectra with the use of Eqs. 10 and 11, and Eq. 13 will relate the computed absorption index spectrum, κ, to the spectral absorption coefficient, k.

An alternative to using a harmonic oscillator model to compute the optical constant spectra is to compute them from a measured transmission[15] or attenuated total reflectance spectrum.[16] Ohta and Ishida have described a matrix formalism for the analysis of light beam intensity in stratified multilayered films that produces equivalent results to the radiative transfer theory.[17,18]

EXPERIMENTAL

All emission and absorption measurements were made with the use of a Perkin-Elmer 1720 FT-IR modified for emission measurements. Surface cooling of the sample was accomplished by applying a pulsed or continuous flow of room-temperature or liquid nitrogen-cooled helium from a 0.32-cm-i.d. copper tube positioned approximately 2 cm away from the sample surface. Material used for the solid analysis was a copolymer of ethylene and vinyl acetate, Elvax®, and for the liquids analysis a silicone oil (dimethyl silicone fluid, Thomas® Scientific) and a polyol (Niax E474, Union Carbide) were used to simulate viscous fluid samples. Temperature measurements for the polymer analyses were made with the use of a thermocouple inserted into an aluminum block that was used for heating the polymer. This device was attached to a temperature controller, and it is estimated that the temperature in the block was controlled to within 1°C. For the fluid analyses, the thermocouple was simply placed in the fluid to measure the temperature, and a hot plate was used for heating. Emission spectra simulations were performed with the use of the Matlab computing environment (The MathWorks, Inc., Natick, MA).

RESULTS AND DISCUSSION

Simulations. In order to investigate the spectral behavior under varying experimental conditions—conditions that may not be readily available due to instrumental limitations—simulations were performed with the use of the models discussed in the Theory section. The

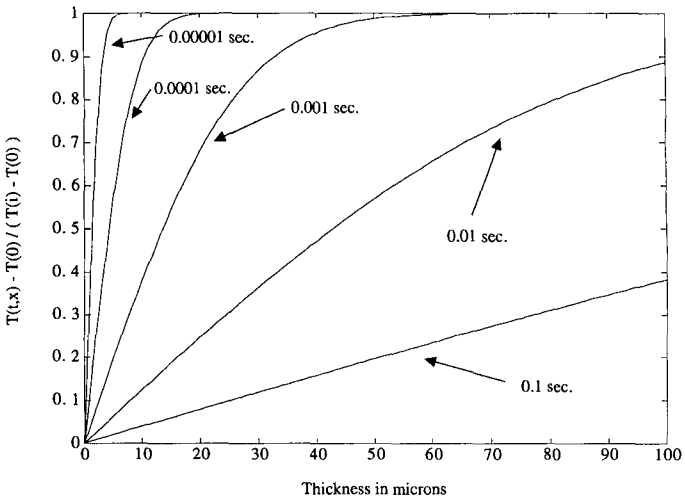

FIG. 2. Temperature distribution as a function of time and position for a thermal diffusivity of 2 × e-7 m²/s.

harmonic oscillator parameters used to generate the optical constant spectra are as follows:

$B = 30{,}000\ \text{cm}^{-2}$	(Oscillator strength)
$\gamma = 20\ \text{cm}^{-1}$	(Damping coefficient)
$\nu_0 = 1730\ \text{cm}^{-1}$	(Resonance frequency)
$n = 1.5$	(Refractive index from the visible)

Spectral range = 2000 − 1500 cm^{-1} at 5-cm^{-1} intervals.

These parameters generate a maximum of about 0.4 in the absorption index spectrum at 1730 cm^{-1}, which is reasonable for an organic material.[14] Temperature-gradient simulations were computed with the use of a thermal diffusivity of 2 × 10^{-7} m²/s, typical of polymeric materials.[19] Figure 2 displays the temperature gradient profiles, $(T(x, \tau) - T_0)/(T_i - T_0)$, as a function of time and position for such a material. As can be seen, the temperature gradient is fairly short lived, in that the temperature at 15 μm is half way to the lower temperature value in 10^{-3} s, indicating the need for rapid spectral measurement or scan synchronization with the thermal pulsing.

Figure 3 displays simulated IRE-TC spectra for a 4 K temperature drop from 323 to 319 K observed at 10^{-5}, 10^{-3}, 10^{-2}, 0.1, 1, and 10 s after cooling begins. This temperature drop was found to occur in the experimental studies described later. The signal increases as the time difference between cooling and observation increases, but the spectral features also tend to broaden with longer time differences, indicating an increasingly larger optical path as the temperature gradient diffuses into the material. From this simulation it would appear that 10^{-3} s would be a reasonable delay time. The optimal observation time will depend on the thermal properties of the material as well as the temperature drop induced by the cooling.

Figure 4 displays simulated IRE-TC spectra at a constant temperature difference of 4 K, at a constant observation time of 10^{-3} s, and at various upper and lower temperatures. These results indicate that better spectral contrast is found at a lower absolute temperature for the

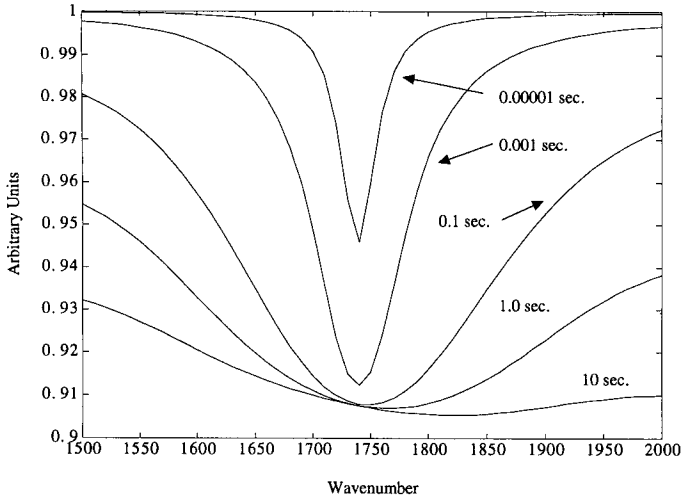

FIG. 3. IRE-TC spectra at constant 4 K temperature drop observed at different times after pulsing.

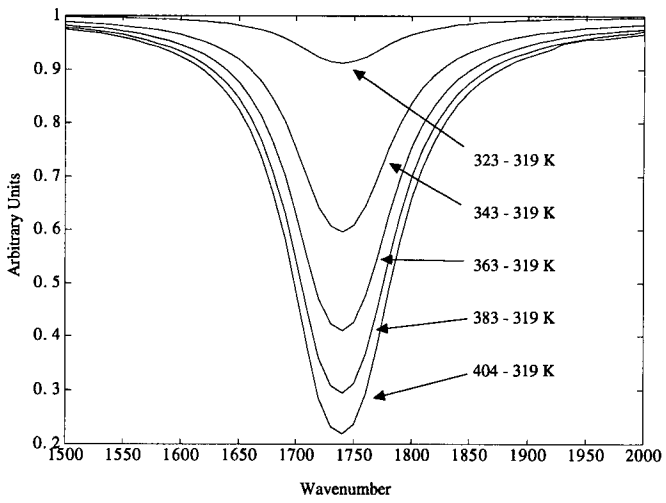

FIG. 5. IRE-TC spectra at constant lower temperature with increasing higher temperature observed at 10^{-3} s.

same temperature difference. Further decreases in the absolute temperature show further improvement in the spectral distinction until the spectral feature begins to show zero transmission at the peak of the band at about 40 K. These results are reasonable if one realizes that the IRE-TC spectrum is a ratio of two spectral measurements and that, at lower absolute temperatures, this relative spectrum (the IRE-TC spectrum) is more well defined because the absolute magnitude of the individual spectra (background and analytical signal) is smaller and, thus, the relative signal is larger. In practice there will be experimental limitations to the extent to which extremely weak signals at low absolute temperatures are detectable. Also, larger temperature drops will be more readily achieved for higher starting temperatures and, thus, would argue for higher absolute temperature experiments. One should exercise caution when considering higher absolute temperature experiments because of the possibility of sample decomposition or degradation.

To investigate this point, we performed a simulation in which the lower temperature was held constant while the upper temperature was increased, resulting in an increase in the temperature drop with a constant time of observation of 10^{-3} s. Figure 5 displays the results. As may be seen, better spectral contrast is found for a larger temperature difference. The extent to which this contrast can be improved will depend on the thermal properties of the materials being studied and the effectiveness of the cooling gas to transport energy away from the surface.

In order to investigate the change in IRE-TC response with concentration, the absorption index spectrum was multiplied by factors less than or equal to 1, generating spectra representative of changing concentrations of a pure component. Figure 6 displays the spectral feature as the factor is changed from 0.01 to 1 for a constant temperature drop from 323 to 319 K and constant observation time of 10^{-3} s. The response is a monotonic function of concentration, but, as shown in Fig. 7, the response is quite nonlinear. Because the IRE-TC measurement is similar to a transmission measurement, the nonlinear behavior is not unexpected. The curvature of the response vs. concentration is a function of the observation time, with a more linear behavior observed at

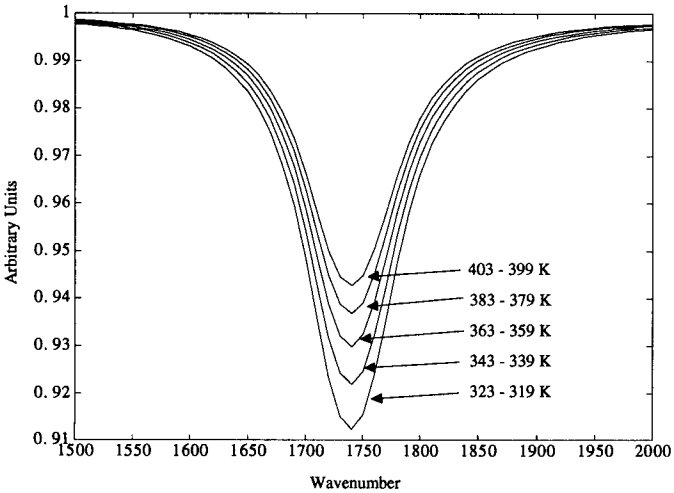

FIG. 4. IRE-TC spectra at constant 4 K temperature drop, constant observation time of 10^{-3} s, and varying upper and lower temperatures.

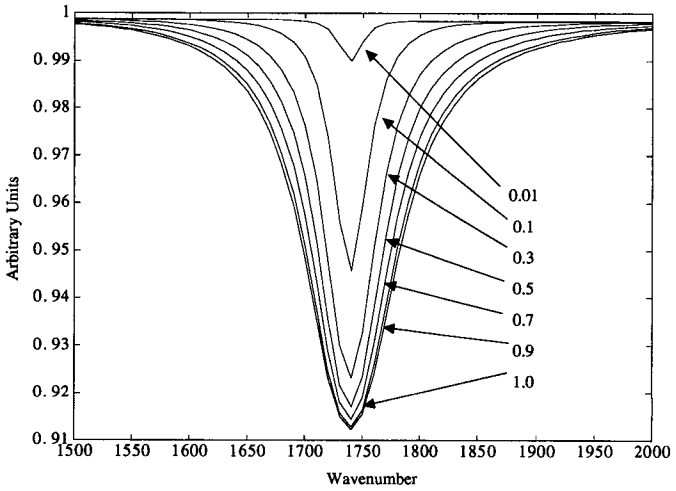

FIG. 6. Spectra as a function of changing concentrations.

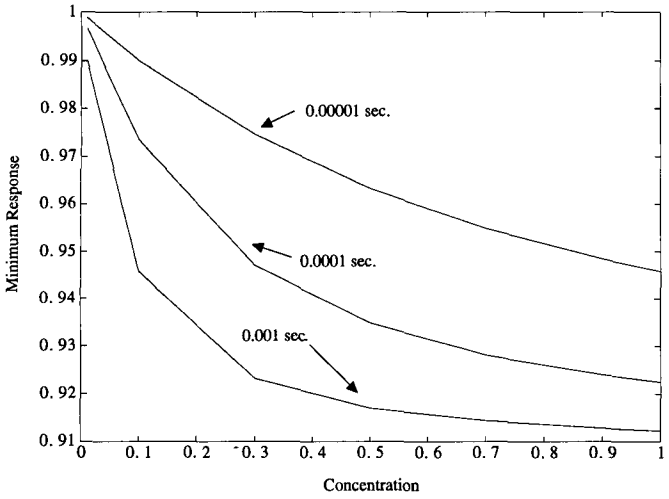

FIG. 7. Minimum response as a function of concentration.

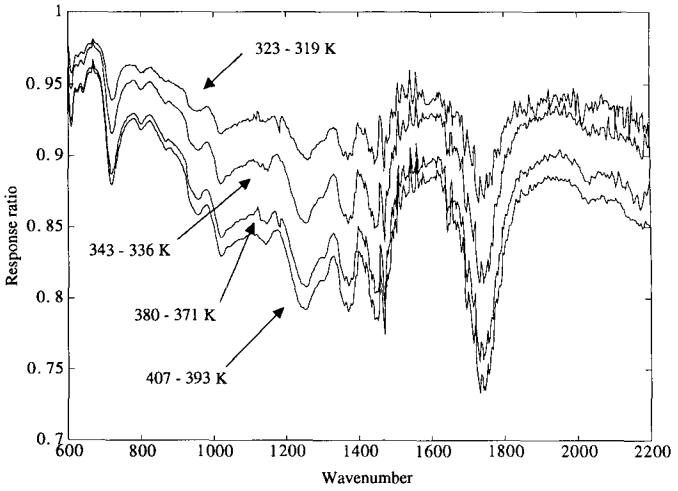

FIG. 9A. Elvax® at different temperature drops and absolute temperatures.

shorter observation times. Several different transformations of the data (such as log of concentration, log of response, and log of both) were tried in order to linearize the univariate relationship. Some linearization was found for the response vs. log(conc) transform at low concentration values. In a process situation, if the process is under control, the deviations would be expected to be small, and thus local linear regions may be available, which would allow modeling of the signal. Multivariate techniques can accommodate a certain amount of nonlinear behavior and have been shown to be useful for the analysis of transient infrared transmission spectroscopy data[10] and standard emission spectra[20] collected from polymer materials. A locally weighted multivariate calibration approach would be reasonable for large nonlinear effects.[21]

Experimental Observations. The need for rapid scanning in order to collect a spectrum in a transiently cooled experiment, as indicated by the spectral simulations, was found to be the case experimentally. The instrument used could scan at a maximum rate of 1 cycle per second, and thus scanning and concurrent pulsing of the gas stream was found to give the best results. Manual synchronization of the pulse and scan limited the reproducibility of these experiments. Figure 8 displays the IRE-TC spectrum of a 1.85-mm-thick Elvax® sample (25% vinyl acetate), at an initial temperature of 373 K, cooled with a one-second pulse of liquid nitrogen-cooled helium with a single scan collected concurrently with the gas pulse. The transmission spectrum of a similar material, but much thinner (~50 μm), measured in the standard transmission mode is also displayed in Fig. 8. Good agreement in the positions of the band minima is observed; however, the peaks in the IRE-TC spectrum appear to be much more saturated than the transmission measurement. The strong C=O stretching band (approx. 1750 cm^{-1}) and CH stretching bands (2700–2900 cm^{-1}) appear highly saturated, and the low absorptivity combination bands at 2000–2240 cm^{-1} are of significant intensity in the IRE-TC spectrum and thus may be useful in quantitative analysis. These features indicate that the effective pathlength, related to the thickness of the cooled layer, is significantly larger than the thickness of the transmission sample. Jones and McClelland found similar results in their investigation of solid samples and demonstrated that, if the sample was rotated faster, a

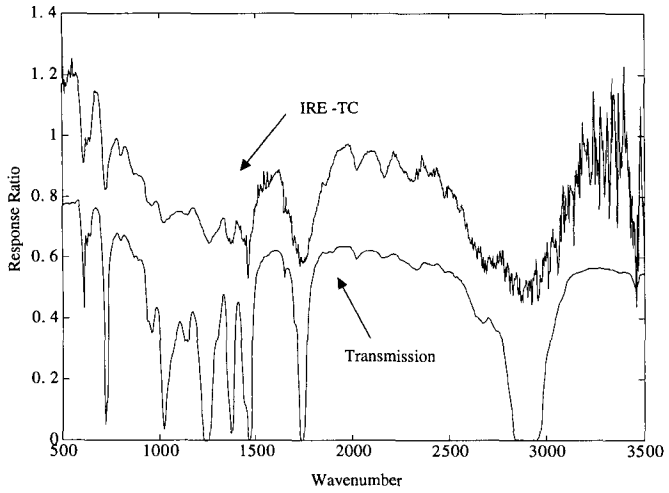

FIG. 8. Elvax® transitively cooled and transmission spectra compared.

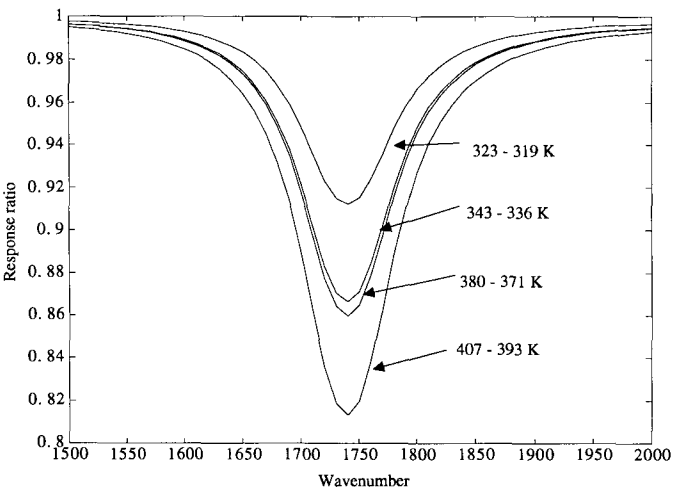

FIG. 9B. Simulation of experimental results in Fig. 9A.

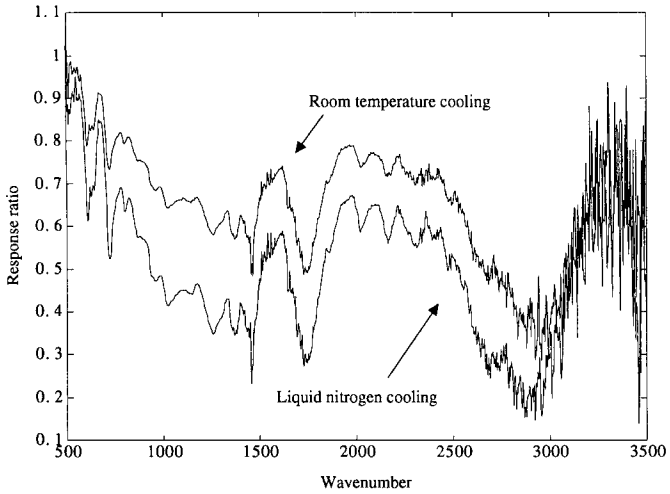

FIG. 10. Elvax® room-temperature and liquid nitrogen-cooled He cooling.

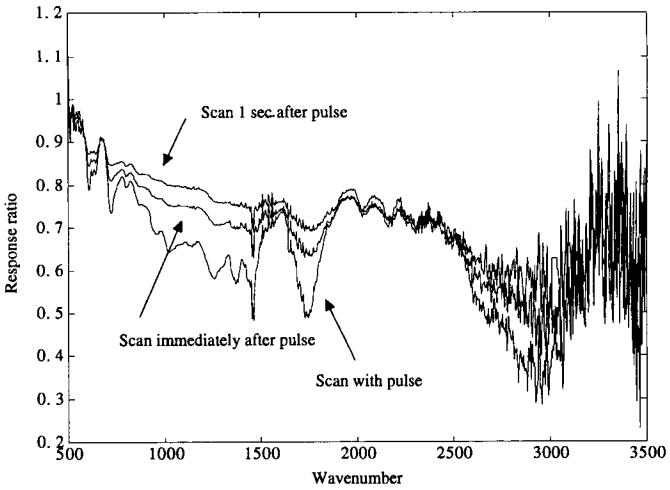

FIG. 11. Elvax® at different scan times after pulsing with coolant.

thinner chilled layer was produced, as evidenced by less saturation in the observed spectra.[10]

Other features to note are the poor signal-to-noise ratio at the high-wavenumber region of the IRE-TC spectrum due to the fall off in the Planck law intensity at higher energy regions of the spectrum. Uncompensated water vapor absorptions in the 1500–2000 cm^{-1} region are also apparent as the result of displacement of water from the beam path by the cooling jet pulse. The sharp feature at 1450 cm^{-1} is an instrumental anomaly believed to be associated with the beamsplitter coating. If the instrumentation were able to scan more quickly or if the scan time could be properly and precisely synchronized with the cooling gas pulses, much sharper spectral features might be expected.

Figure 9A displays four spectra of an Elvax® sample (18% vinyl acetate, 0.95 mm thick) collected under various temperature drop conditions. The water vapor displaced in the optical path due to the cooling pulse is very prominent. The higher initial temperature and larger temperature drop experiments have a better signal-to-noise ratio, evident in the 2000–2200 cm^{-1} region. Also note the better spectral definition of the 1750-cm^{-1} band for the larger-temperature-drop experiments. Figure 9B displays simulations with the same temperatures as the experiment. As the temperature difference increases, better spectral contrast is observed, and the overall spectral baseline shifts down—consistent with the theoretical results.

The effect of the temperature of the coolant gas was investigated by pulsing the 1.85-mm Elvax® sample initially at 70°C with room-temperature and liquid nitrogen-cooled helium for one second with concurrent spectral scanning. The results are displayed in Fig. 10. The liquid nitrogen-cooled spectrum shows a lower overall baseline, indicating a lower transient temperature and greater spectral contrast for many spectral features. Although there are some advantages for the liquid nitrogen-cooled helium pulse, these may not be significant when the other experimental difficulties inherent with this approach are considered. These difficulties include condensation of water vapor and CO_2 on the sample surface and displacement of water and CO_2 from the optical path by evaporating liquid nitrogen coolant.

The lifetime of the temperature gradient must be quite short, as indicated by the rapid propagation of the temperature distribution in the simulation studies and the need to scan with the cooling pulse for the best results experimentally. Three experiments were conducted in which the scan of the spectrometer was started concurrently with the pulse, immediately after the pulse, and 1 s after the pulse in order to estimate the gradient lifetime. The results are displayed in Fig. 11. As can be seen, the spectral features are reduced to a great extent, even for the spectrum collected immediately after the pulse, as the gradient loses definition in a relatively short time in comparison to the maximum scan speed of the instrument. Accurate determination of the gradient lifetimes will be important for proper pulse scan synchronization experiments.

Attempts to apply continuous cooling and scanning of the polymer samples resulted in a better signal-to-noise ratio but also in greater saturation and less spectral definition. Because the experimental arrangement did not allow for rotation of the sample, as in the work of Jones

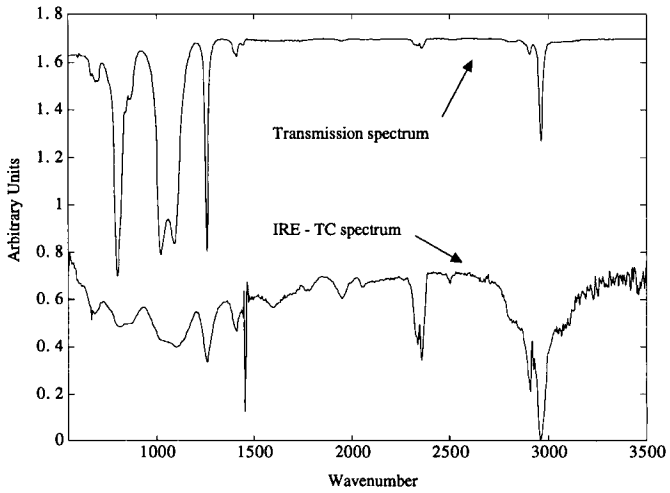

FIG. 12. Silicone oil transmission and best emission measurements.

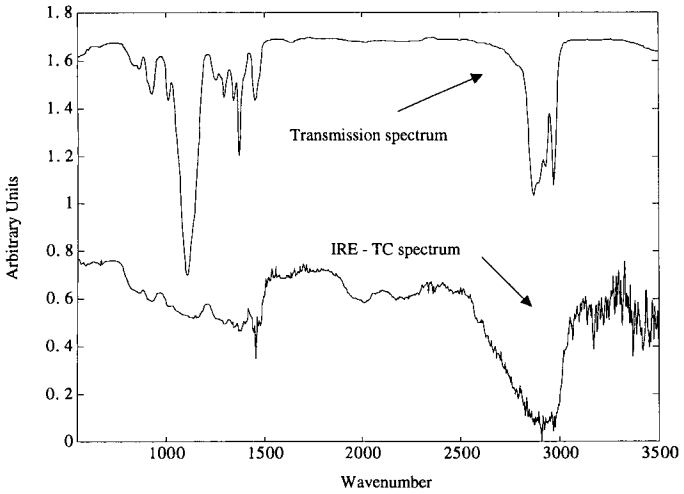

FIG. 13. Niax transmission and best absorption.

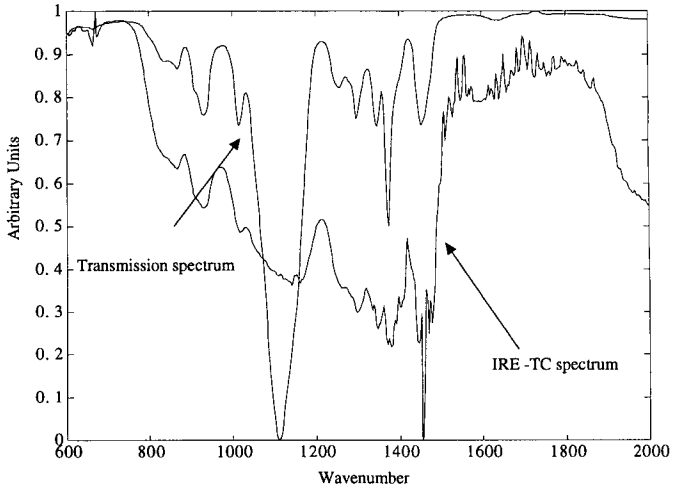

FIG. 14. Detailed features from Niax spectrum in the range 600 to 2001 cm^{-1}.

and McClelland,[10] we decided to investigate the analysis of liquid samples. We reasoned that a sharper temperature gradient might be maintained by cooling a fluid, because the cooled surface layer could be quickly replaced by hotter fluid before a thicker, more diffuse temperature gradient could be formed. Figure 12 displays the scaled and offset transmission and IRE-TC spectra of a silicone oil. The silicone oil is at 463 K with room-temperature helium flowing continuously with continuous scanning for 10 min and no stirring (stirring did not change the observed spectral feature significantly). As can be seen, the spectral features correspond quite well between the two spectra, but there is noticeable saturation in the IRE-TC spectrum. Due to signal averaging, a noise reduction for the higher-wavenumber region of the spectrum, relative to the spectra displayed earlier, is noted. Therefore, again, spectral saturation is observed for the liquid sample when compared with the thin-film transmission measurement. However, there is still some structure available, and this might be sufficient for process analysis. It is also possible that this method is the only way to obtain relevant information from hot opaque samples in a convenient and safe manner.

Figure 13 displays the scaled and offset transmission and IRE-TC spectrum for a Niax polyol sample at 413 K, with stirring. The spectral features are very saturated when compared with the transmission spectrum of a thin film. However, a more detailed inspection of the 600–2001 cm^{-1} region, shown in Fig. 14, indicates that there is still some structure present in the IRE-TC spectrum. These spectral data may be sufficient for monitoring processes, which are expected to take place at relatively constant set points and thus do not need a wide dynamic range for the sensor response.

CONCLUSIONS

In summary, a theory is developed for IRE-TC using unsteady heat flow calculation to define a temperature gradient, a harmonic oscillator model to compute optical constant spectra, and a radiation transfer theory to simulate spectral features from a sample with an imposed temperature gradient. For typical polymer materials, simulations indicate that the temperature gradient is quite short lived, and thus so too are the spectral features associated with the gradients; this observation was confirmed experimentally. There is qualitative agreement between theory and experiment. Experimental data that are in better agreement with theory might be obtained with faster scanning and more precise control over the pulse scan synchronization, and through the use of the approach by Ohta and Ishida, in which the optical constant spectra are estimated from measured absorption spectra.

Infrared emission spectra with transient cooling were measured for solids and liquids samples and were found to be significantly saturated when compared with thin-film transmission spectra. Even in the case of very saturated spectra, these results may be sufficient for a process analysis situation in which a large dynamic range is not necessary and a simple, rapid analytical method is needed.

ACKNOWLEDGMENTS

R.J.P. acknowledges the support of a fellowship sponsored by the Dow Chemical Company and an ACS Analytical Division Fellowship sponsored by the Perkin-Elmer Corporation and the American Chemical Society Analytical Division. This work was supported by the Center for Process Analytical Chemistry (CPAC), a National Science Foundation Industry/University Cooperative Research Center at the University of Washington.

1. D. B. Chase, Appl. Spectrosc. **35,** 77 (1981).
2. M. J. D. Low and I. Coleman, Spectrochim. Acta **22,** 369 (1966).
3. N. Sheppard, "The Use of Fourier Transform Methods for the Measurement of Infrared Emission Spectra," in *Analytical Applications of FT-IR to Molecular and Biological Systems,* Proceedings of the 1979 NATO Advanced Study Institute, J. R. Durig, Ed. (D. Reidel Publishing Company, Dordrecht, Holland, 1980), p. 125.
4. S. F. Kapff, J. Chem. Phys. **16,** 446 (1948).
5. O. Koga, T. Onishi, and K. Tamaru, J.C.S. Chem. Comm., 464 (1974).
6. R. W. Jones and J. F. McClelland, Anal. Chem. **61,** 1810 (1989).
7. R. W. Jones and J. F. McClelland, Anal. Chem. **61,** 650 (1989).
8. L. T. Lin, D. D. Archibald, and D. E. Honigs, Appl. Spectrosc. **42,** 477 (1988).
9. R. W. Jones and J. F. McClelland, Anal. Chem. **62,** 2047 (1990).
10. R. W. Jones and J. F. McClelland, Anal. Chem. **62,** 2247 (1990).

11. J. Hvistendahl, E. Rytter, and H. A. Oye, Appl. Spectrosc. **37,** 182 (1983).
12. J. P. Holman, *Heat Transfer* (McGraw-Hill Book Company, New York, 1986), 6th ed., p. 131.
13. J. L. Lauer and V. W. King, Infrared Phys. **19,** 395 (1979).
14. P. J. Hommert, R. Viskanta, and R. E. Chupp, J. Am. Ceram. Soc. **58,** 58 (1975).
15. R. T. Graf, J. L. Koenig, and H. Ishida, Appl. Spectrosc. **39,** 405 (1985).
16. K. Ohta, R. T. Graf, and H. Ishida, Appl. Spectrosc. **42,** 114 (1988).
17. K. Ohta and H. Ishida, Appl. Opt. **29,** 1952 (1990).
18. K. Ohta and H. Ishida, Appl. Opt. **29,** 2466 (1990).
19. E. V. Thompson, "Thermal Properties," in *Encyclopedia of Polymer Science and Engineering,* J. I. Kroschqitz, Ed. (John Wiley and Sons, New York, 1985), Vol. 16, p. 711.
20. R. J. Pell, B. C. Erickson, R. W. Hannah, J. B. Callis, and B. R. Kowalski, Anal. Chem. **60,** 2824 (1988).
21. T. Næs, T. Isaksson, and B. R. Kowalski, Anal. Chem. **62,** 664 (1990).